The Journal of Immunology

IFN-γ-Inducible Protein 10 (IP-10; CXCL10)-Deficient Mice Reveal a Role for IP-10 in Effector T Cell Generation and Trafficking

Jennifer H. Dufour, Michelle Dziejman, Michael T. Liu, Josephine H. Leung, Thomas E. Lane and Andrew D. Luster

J Immunol 2002; 168:3195-3204; ;
doi: 10.4049/jimmunol.168.7.3195
http://www.jimmunol.org/content/168/7/3195

The Journal of Immunology is published twice each month by
The American Association of Immunologists, Inc.,
1451 Rockville Pike, Suite 650, Rockville, MD 20852

Print ISSN: 0022-1767 Online ISSN: 1550-6606.

IFN-γ-Inducible Protein 10 (IP-10; CXCL10)-Deficient Mice Reveal a Role for IP-10 in Effector T Cell Generation and Trafficking[1]

Jennifer H. Dufour,[2]* Michelle Dziejman,[3]* Michael T. Liu,† Josephine H. Leung,* Thomas E. Lane,† and Andrew D. Luster[4]*

IFN-γ-inducible protein 10 (IP-10, CXCL10), a chemokine secreted from cells stimulated with type I and II IFNs and LPS, is a chemoattractant for activated T cells. Expression of IP-10 is seen in many Th1-type inflammatory diseases, where it is thought to play an important role in recruiting activated T cells into sites of tissue inflammation. To determine the in vivo function of IP-10, we constructed an IP-10-deficient mouse (IP-10$^{-/-}$) by targeted gene disruption. Immunological analysis revealed that IP-10$^{-/-}$ mice had impaired T cell responses. T cell proliferation to allogeneic and antigenic stimulation and IFN-γ secretion in response to antigenic challenge were impaired in IP-10$^{-/-}$ mice. In addition, IP-10$^{-/-}$ mice exhibited an impaired contact hypersensitivity response, characterized by decreased ear swelling and reduced inflammatory cell infiltrates. T cells recovered from draining lymph nodes also had a decreased proliferative response to Ag restimulation. Furthermore, IP-10$^{-/-}$ mice infected with a neurotropic mouse hepatitis virus had an impaired ability to control viral replication in the brain. This was associated with decreased recruitment of CD4$^+$ and CD8$^+$ lymphocytes into the brain, reduced levels of IFN-γ and the IFN-γ-induced chemokines monokine induced by IFN-γ (Mig, CXCL9) and IFN-inducible T cell α chemoattractant (I-TAC, CXCL11) in the brain, decreased numbers of virus-specific IFN-γ-secreting CD8$^+$ cells in the spleen, and reduced levels of demyelination in the CNS. Taken together, our data suggest a role for IP-10 in both effector T cell generation and trafficking in vivo. ***The Journal of Immunology*****, 2002, 168: 3195–3204.**

We initially identified human IFN-γ-inducible protein of 10 kDa (IP-10/CXCL10)[5] as an early response gene induced by IFN-γ in U937 cells (a monocyte-like cell line) (1). IP-10 is constitutively expressed at low levels in thymic, splenic, and lymph node stroma (2). However, expression can be highly induced in a variety of cells, including endothelial cells, keratinocytes, fibroblasts, mesangial cells, astrocytes, monocytes, and neutrophils by stimulation with IFN-α, IFN-β, IFN-γ, or LPS and in T cells by Ag activation (3–5). IP-10 is also expressed in many Th1-type human inflammatory diseases, including skin diseases (e.g., psoriasis) (6, 7), multiple sclerosis (8, 9), atherosclerosis (10), rheumatoid arthritis (11), transplant rejection (12, 13), and inflammatory bowel diseases (14). Elevated levels of IP-10 protein have been found in the cerebral spinal fluid in patients with viral meningitis (15) and multiple sclerosis (8), in the bronchoalveolar lavage fluid of patients with pulmonary sarcoidosis (16) and lung transplantation undergoing rejection (13), and in the serum of patients with chronic active hepatitis (17). In these diseases, levels of IP-10 correlate with the tissue infiltration of T lymphocytes, suggesting that IP-10 plays an important role in the recruitment of T cells to sites of inflammation.

IP-10 is structurally and functionally related to monokine induced by IFN-γ (Mig, CXCL9) and IFN-inducible T cell α chemoattractant (I-TAC, CXCL11). These three chemokines direct migration and stimulate the adhesion of activated T cells and NK cells by binding to and activating CXCR3, a G protein-coupled receptor. CXCR3 is expressed on activated T cells, preferentially of the Th1 phenotype, on NK cells, and on a significant fraction of circulating CD4$^+$ and CD8$^+$ T cells (~20–40%) (18–20). The majority of peripheral CXCR3$^+$ T cells express CD45RO (memory T cells) as well as β_1 integrins (20), which are implicated in the binding of lymphocytes to endothelial cells and the extracellular matrix (21). In addition, CXCR3 has been reported to be expressed on plasmacytoid and myeloid dendritic cells (22, 23), leukemic B cells (24, 25), eosinophils (26), dividing microvascular endothelial cells (27, 28), thymocyte subsets (29), and GM-CSF-treated CD34$^+$ cord blood cells (30).

Among the CXC chemokines, IP-10, Mig, and I-TAC are unique in that they are all induced by IFN-γ in a wide variety of cell types (3, 10, 31, 32) and act through the chemokine receptor CXCR3. However, while these three ligands activate the same receptor, it is becoming clear that they exhibit unique expression

*Center for Immunology and Inflammatory Diseases, Division of Rheumatology, Allergy and Immunology, Massachusetts General Hospital, Harvard Medical School, Boston, MA 02114; and †Department of Molecular Biology and Biochemistry, University of California, Irvine, CA 92697

Received for publication October 16, 2001. Accepted for publication January 25, 2002.

The costs of publication of this article were defrayed in part by the payment of page charges. This article must therefore be hereby marked *advertisement* in accordance with 18 U.S.C. Section 1734 solely to indicate this fact.

[1] This work was supported by National Institutes of Health Grants F32CA88721 (to J.H.D.), F32AI09716 (to M.D.), NS37336-01 (to T.E.L.), and RO1CA69212 (to A.D.L.). M.T.L. was supported in part by National Institutes of Health Training Grant T32NSO74444. T.E.L. was also supported by National Multiple Sclerosis Society Grant RG30393A1/T).

[2] Current address: Section of Pulmonary and Critical Care, Yale University School of Medicine, New Haven, CT 06520.

[3] Current address: Department of Microbiology and Molecular Genetics, Harvard Medical School, Boston, MA 02114.

[4] Address correspondence and reprint requests to Dr. Andrew D. Luster, Center for Immunology and Inflammatory Diseases, Division of Rheumatology, Allergy and Immunology, Massachusetts General Hospital, Building 149, 13th Street, Charlestown, MA 02129. E-mail address: luster@helix.mgh.harvard.edu

[5] Abbreviations used in this paper: IP-10, IFN-γ-inducible protein 10; DNFB, 2,4-dinitro-1-fluorobenzene; DNBS, dinitrobenzene sulfonate; ES, embryonic stem; i.c., intracranial(ly); I-TAC, IFN-inducible T cell α chemoattractant; LFB, Luxol fast blue; MCP, monocyte chemoattractant protein; MHV, mouse hepatitis virus; Mig, monokine induced by IFN-γ; p.i., postinfection.

0022-1767/02/$02.00

patterns in vivo, and experiments using neutralizing Abs and gene-targeted mice support the concept that these three chemokines may have nonredundant functions in vivo. Compared with Mig and I-TAC, IP-10 expression is seen earlier following infection with a variety of pathogens and in response to LPS injection (33–35). In addition, differential expression of IP-10, Mig, and I-TAC has been demonstrated in human atherosclerotic lesions in situ (10) and in several skin diseases, including psoriasis (7, 36). mAb neutralization demonstrated that IP-10 is required for survival following infection of mice with *Toxoplasma gondii* (34) and cannot be substituted by other CXCR3 chemokine ligands. Neutralization of IP-10 inhibited T cell infiltration into infected tissues and impaired Ag-specific T cell effector functions, resulting in a massive increase in tissue parasite burden, leading to increased mortality. Ab neutralization of IP-10 has also been shown to block the recruitment of effector T cells into the CNS in a passive transfer model of murine experimental autoimmune encephalomyelitis (37). In addition, in a murine viral hepatitis model with both acute and chronic stages of CNS inflammation and injury, neutralization of IP-10 increased mortality and delayed viral clearance from the CNS in the acute phase (38). This was associated with reduced effector T cell recruitment into the brain. In addition, in the chronic phase anti-IP-10 treatment inhibited progression of demyelination, increased remyelination, and improved neurological function (39). Interestingly, anti-Mig treatment had no effect on the chronic phase of the illness, confirming that IP-10 and Mig can subserve different biological functions in vivo. This has also been suggested by studies that revealed that Ab neutralization of Mig inhibited T cell infiltration into class II MHC-disparate murine skin allografts and inhibited acute rejection (40). This concept is further supported by our recent studies using the IP-10-deficient mice that we describe here, which demonstrated a requirement for allograft-derived IP-10 for the early recruitment of NK cells and T cells into cardiac allografts to initiate acute rejection (41).

In addition to their well-described function of recruiting leukocytes to sites of inflammation, chemokines also play a role in the generation and function of effector cells. In fact, IP-10 has been shown to augment IFN-γ release from PBMC cultures following stimulation with environmental Ags (42). Furthermore, mAb neutralization has also revealed a role for IP-10 in the generation of tumor-specific effector T cells and tumor protective immunity in an IL-12 gene therapy model (43). These data suggest that IP-10 and CXCR3 may play a role in the generation and function of effector T cells, in addition to or as a result of their activity in T cell recruitment.

In this study mice deficient in IP-10 were generated and found to have an impaired response to alloantigen stimulation in MLR assays and reduced T cell responses following primary immunization with exogenous Ag. These mice also exhibited a reduced contact hypersensitivity response and an impaired host immune response to mouse hepatitis virus (MHV) infection that was characterized by decreased generation and tissue recruitment of effector T cells. These data demonstrate that IP-10 plays a role in the generation and delivery of an effector T cell response.

Materials and Methods

Targeted disruption of IP-10

A mouse 129Sv/J genomic library (Stratagene, La Jolla, CA) was screened with a mouse IP-10 cDNA probe (4, 5) to isolate a phage, pλ26, which contained ~20 kb of IP-10 genomic DNA. To disrupt the IP-10 gene, a 5.5-kb *Xba*I (X)-*Eco*RV (RV) fragment that includes only exon 4 was subcloned into PGK-Neo, which contains the gene for neomycin resistance driven by the phosphoglycerate kinase promoter (see Fig. 1). A 2-kb PCR product containing sequences upstream of the IP-10-coding region was generated using murine chromosomal DNA and primers based on the published murine IP-10 gene sequence (44). The upstream primer included a *Sal*I (S) restriction site, and the downstream primer included a *Xho*I (Xh) site. These sites were used to subclone the PCR product into the unique *Sal*I site of the targeting vector. To provide negative selection for a single homologous recombination event, the gene for thymidine kinase, driven by the HSV promoter, was cloned into the targeting vector. The IP-10 targeting vector was used to electroporate J1 embryonic stem (ES) cells and selected for neomycin resistance. 1-(2-Deoxy-2-fluoro-1-β-D-arabinofuranosyl)-5-iodouracil was added, and the resulting clones were picked on day 7 postelectroporation. The frequency of homologous recombination in ES cells was 0.5%. An ES clone containing the disrupted allele was injected into blastocysts and resulted in live births after transfer to a foster mother. The chimeras from this clone passed the disrupted allele to their progeny, which were intercrossed to produce mice homozygous for the disrupted allele. Mice were genotyped by Southern blot analysis of DNA digested with *Xba*I using standard techniques. Using an ~500 bp genomic DNA fragment upstream from the *Xho*I site at the 5′ end of exon 1 as a probe, the wild-type allele generated a 2-kb hybridizing fragment; the disrupted allele generated a larger 2.7-kb fragment. Additional confirmatory Southern blots of ES clones were performed using the neomycin resistance gene as a probe on *Bam*HI-digested DNA and an IP-10 cDNA probe on *Xba*I- or *Sac*I-digested DNA. The initial chimeric mice (129Sv/J ES cell into C57BL/6 blastocyst) were mated back to 129Sv/J mice to introduce the disrupted allele onto a pure 129Sv/J background. IP-10$^{+/+}$ and IP-10$^{-/-}$ mice on a pure 129Sv/J background were used in all experiments, with the exception of the MHV model. For the MHV experiments, (129Sv/J $\times$ C57BL/6)F_1 IP-10$^{-/-}$ and IP-10$^{+/+}$ littermate control mice were used. All mice were used between 6–12 wk of age.

Northern blot analysis

Briefly, bone marrow was flushed from the femurs of mice and cultured for 7 days in the presence of 5 ng/ml M-CSF (PeproTech, Rocky Hill, NJ) in DMEM supplemented with 10% FCS, 2 mM L-glutamine, 100 μg/ml streptomycin, 100 U/ml penicillin, 1 mM sodium pyruvate, and 50 μM β-ME (CD10; Cellgro-Mediatech, Herndon, VA). Bone marrow-derived macrophages were then stimulated with 100 ng/ml IFN-γ or 100 ng/ml LPS in the presence of serum for 5 h, and RNA was isolated using RNA STAT-60 (Tel-Test, Friendswood, TX). RNA was fractionated on a 1.2% agarose gel containing 0.7% formaldehyde, transferred to GeneScreen (DuPont-NEN, Boston, MA) overnight using 10$\times$ SSC, and fixed to the membrane by UV cross-linking (Stratalinker; Stratagene). The membrane was hybridized with [^{32}P]dCTP Klenow-labeled random primed murine cDNA probes for IP-10, Mig (provided by Dr. J. Farber), I-TAC (provided by Dr. G. Werner-Felmayer), KC, and actin as a control for RNA loading. The membrane was hybridized under high stringency conditions (50% formamide, 10% dextran sulfate, 5$\times$ SSC, 1$\times$ Denhardt's solution, 1% SDS, 100 μg/ml denatured herring sperm DNA, and 20 mM Tris at 42°C) and washed at 55°C in 0.2$\times$ SSC and 0.1% SDS.

Western blot analysis

Bone marrow-derived macrophages were stimulated with 100 ng/ml IFN-γ or 100 ng/ml LPS in the presence of serum for 5 h. Macrophages were washed, and stimulants were added in serum-free medium for an additional 48 h. Culture supernatants were collected, clarified by centrifugation, and concentrated using Centricon-3 concentration units (Amicon, Beverly, MA). Samples were resolved on a 12.5% Tris-tricine acrylamide gel and transferred to polyvinylidene difluoride membrane (DuPont-NEN). IP-10 secretion was determined by immunoblotting with rabbit polyclonal antiserum to IP-10 (45) and detection by chemiluminescence (DuPont-NEN). Recombinant murine IP-10 (PeproTech) was used as a control.

Mixed lymphocyte reactions

Responding splenocytes (IP-10$^{+/+}$ or IP-10$^{-/-}$ 129Sv/J, H-2^b or BALB/c, H-2^d) were cultured with 2×10^5 mitomycin C (Sigma-Aldrich, St. Louis, MO)-treated syngeneic or allogeneic splenocytes or Con A (10 μg/ml; Calbiochem, La Jolla, CA) for 6 days at 37°C in a 5% CO_2 atmosphere. Proliferation was determined by incorporation of [*methyl*-^{3}H]thymidine (DuPont-NEN) during the final 18 h of culture.

Response to OVA

Mice were immunized with 100 μg OVA (Sigma-Aldrich) in CFA (Sigma-Aldrich) i.p. Seven days later animals were sacrificed, and serum Ig isotypes were determined using an OVA-specific ELISA (Pierce, Rockford,

IL). A series of serum dilutions was examined in each experiment, and dilutions (1/100) in the linear range of the assay were reported. Lymph nodes were aseptically removed on day 7 postinfection (p.i.), dispersed into single-cell suspensions, and stimulated in the presence or the absence of 50 μg/ml OVA in vitro for 48 h. Proliferation was determined by incorporation of [^{3}H]thymidine. Culture supernatants were collected at 48 h from duplicate cultures and were assayed by ELISA for IFN-γ, IL-4, and IL-5 (Endogen, Woburn, MA).

Contact hypersensitivity response

Mice were sensitized by application of 0.05 ml 0.5% 2,4-dinitro-1-fluorobenzene (DNFB; Sigma-Aldrich) (dissolved in 3/1 acetone/olive oil) to the shaved backs of animals. Six days later, the baseline thickness of the animal's ears was measured using a precision thickness gauge (Mitutoyo, Aurora, IL). Each side of the ear was then treated epicutaneously with 0.01 ml of 0.2% DNFB in acetone, and ear thickness was measured 24 h later. Ear swelling was determined by subtracting prechallenge ear thickness from measurements 24 h postchallenge. For histopathologic analysis, ears were fixed in 10% neutral buffered formalin. Tissues were embedded in paraffin, sectioned, and stained with H&E. For proliferation assays, cervical lymph nodes were removed 24 h postchallenge and dispersed into single-cell suspensions. Cells (2×10^5) were stimulated in vitro in the absence or the presence of 50 μg/ml dinitrobenzene sulfonate (DNBS, soluble analog of DNFB; Sigma-Aldrich) for 48 h. Proliferation was determined by incorporation of [^{3}H]thymidine.

Infection with MHV

IP-10$^{+/+}$ and IP-10$^{-/-}$ mice were injected intracranially (i.c.) with 1000 PFU MHV strain J2.2V-1 suspended in 30 μl sterile saline. Control animals received an i.c. injection of saline alone. To determine viral burden following infection, IP-10$^{-/-}$ and IP-10$^{+/+}$ mice were sacrificed on days 7 and 12 p.i. Brains were removed, and one-half was used for plaque assay on the DBT astrocytoma cell line as previously described (46). The remaining halves of brain were used for immunophenotyping the cellular infiltrate by flow cytometry using a previously published protocol (46). FITC-conjugated Abs to CD4 and CD8 (BD PharMingen, San Diego, CA) were used to detect infiltrating T lymphocytes. FITC-conjugated F4/80 (Serotec, Oxford, U.K.) was used to detect activated macrophages/microglial cells. For RT-PCR analysis, total RNA was extracted from brains of mice at 7 days p.i. using TRIzol reagent (Life Technologies, Gaithersburg, MD) and were reverse transcribed using the AMV reverse transcriptase system (Promega, Madison, WI). PCR amplification was performed on the resulting cDNA for 30 cycles with specific primers for L32 (forward, 5′-AACGCTCAGCTCCTTGACAT; reverse, 5′-AACCCAGAGGCATTGACAAC), Mig (forward, 5′-CGTCGTCGTTCAAGGAAG; reverse, 5′-TCGAAAGCTTGGGAGGTT), I-TAC (forward, 5′-GCGGCCGCGAGGACGCTGTCTTTGCATAGG; reverse, 5′-GAATTCAGCCTTGCTTGCTTCGATTTGG), or IFN-γ (Clontech Laboratories, South San Francisco, CA). Sequence analysis of L32, Mig, and I-TAC amplicons confirmed primer specificity. Amplification was performed on an automated PerkinElmer/Cetus (Norwalk, CT) model 480 DNA thermocycler using the following profile: step 1, initial denaturation at 94°C for 45 s; step 2, annealing at 60°C for 45 s; and step 3, extension at 72°C for 2 min. Steps 1–3 were repeated 29 times for a total of 30 cycles and were followed by a 7-min incubation at 72°C.

LFB staining of spinal cords and analysis by light microscopy

Demyelination was scored on spinal cords stained with Luxol fast blue (LFB). Demyelination was scored as follows: 0, no demyelination; 1, mild inflammation accompanied by loss of myelin integrity; 2 moderate inflammation with increasing myelin damage; 3, numerous inflammatory lesions accompanied by significant increase in myelin stripping; and 4, intense areas of inflammation accompanied by numerous phagocytic cells engulfing myelin debris (46). Scores were averaged and are presented as the average ± SEM.

Intracellular cytokine staining

Intracellular cytokine staining was performed using a previously described procedure (47). In brief, IP-10$^{+/-}$ and IP-10$^{-/-}$ mice were infected i.p. with 2×10^5 PFU MHV-4. Splenocytes were isolated at 8 days p.i. and pooled, and 1×10^6 total cells were stimulated with peptide corresponding to the CD8 epitope in the surface (S) glycoprotein spanning residues 510–518 (S510–518) (48, 49). After incubation for 6 h at 37°C in medium containing Golgi stop (Cytofix/Cytoperm kit; BD PharMingen), cells were washed, and blocked with PBS containing 10% FBS and a 1/200 dilution of CD16/32 (BD PharMingen). Cells were then stained for surface Ags with either FITC-conjugated CD8 or rat IgG2b (as control) for 45 min at 4°C and stained for intracellular IFN-γ using PE-conjugated anti-IFN-γ (1/50; XMG1.2; BD PharMingen) for 45 min at 4°C. Cells were analyzed on a FACStar (BD Biosciences, Mountain View, CA). Data are presented as the percentage of positive cells within the gated population. The absolute numbers of activated CD8$^+$ T lymphocytes was calculated by multiplying the fraction of dual-positive cells by the total number of cells obtained from the spleen.

Statistical analysis

Data were analyzed by Student's *t* test (two-tailed, paired). A value of $p < 0.05$ was considered significant.

Results

Targeted disruption of the IP-10 gene

Mice deficient in IP-10 were generated by targeted gene deletion mutagenesis (Fig. 1). A targeting vector (Fig. 1*A*) was designed that would delete exons 1–3, virtually the entire coding region of IP-10. The targeting vector was electroporated into J1 ES cells and selected for neomycin resistance. An ES clone containing the disrupted allele was injected into blastocysts and resulted in live births after transfer to a foster mother. The chimeras from this clone passed the disrupted allele to their progeny, which were intercrossed to produce mice homozygous for the disrupted allele. Mice were genotyped by Southern blot analysis using a genomic DNA fragment 5′ of exon 1 as a probe (Fig. 1*B*). The wild-type allele generated a 2-kb hybridizing fragment, and the disrupted allele generated a larger 2.7-kb fragment.

To confirm that IP-10 expression had been disrupted, Northern blot analysis was performed (Fig. 1*C*). IP-10$^{-/-}$ mice expressed no detectable mRNA for IP-10 following IFN-γ or LPS stimulation compared with prominent IP-10 mRNA expression in wild-type (IP-10$^{+/+}$) and heterozygous (IP-10$^{+/-}$) mice. The expression of other CXC chemokine genes that cluster with IP-10 on murine chromosome 5, such as Mig, I-TAC, and KC was not affected in IP-10$^{-/-}$ mice (Fig. 1*C*). IP-10 protein secretion was measured in IFN-γ- or LPS-activated bone marrow-derived macrophage cultures by immunoblotting culture supernatants with an affinity-purified rabbit polyclonal anti-serum to IP-10 (Fig. 1*D*). This analysis demonstrated the absence of IP-10 secretion by macrophages derived from IP-10$^{-/-}$ compared with IP-10$^{+/+}$ and IP-10$^{+/-}$ mice.

IP-10$^{-/-}$ mice were born at the expected Mendelian ratios, showed no overt developmental or morphological abnormalities, and were fertile. Immunophenotyping of leukocyte subsets by flow cytometry from spleen, lymph node, thymus, bone marrow, and peripheral blood of IP-10$^{-/-}$ mice using mAbs directed against the neutrophil marker GR-1, the macrophage marker F4/80, the B cell marker B-220, and the T cell markers CD3, CD4, CD8, and CD25 were similar between wild-type and IP-10$^{-/-}$ mice (at least three animals tested for each genotype for each site in three separate experiments; data not shown).

Decreased responses to alloantigen in IP-10$^{-/-}$ mice

The MLR is a model of T cell responsiveness to allogeneic MHC Ags and has been used to investigate the pathways of T cell proliferation. Additionally, the MLR response potentially reflects the activation pathway in acute allograft rejection. We analyzed the generation of an allospecific proliferative response using naive IP-10$^{-/-}$ and IP-10$^{+/+}$ (H-2^b) and BALB/c splenocytes (H-2^d) as both stimulators and responders. Splenocytes from IP-10$^{-/-}$ mice exhibited a significantly reduced proliferative response compared with IP-10$^{+/+}$ responses (~68% reduced; $p = 0.021$; Fig. 2*A*), while the proliferative response to the mitogen Con A was unaffected. In contrast, splenocytes from IP-10$^{-/-}$ and IP-10$^{+/+}$ mice

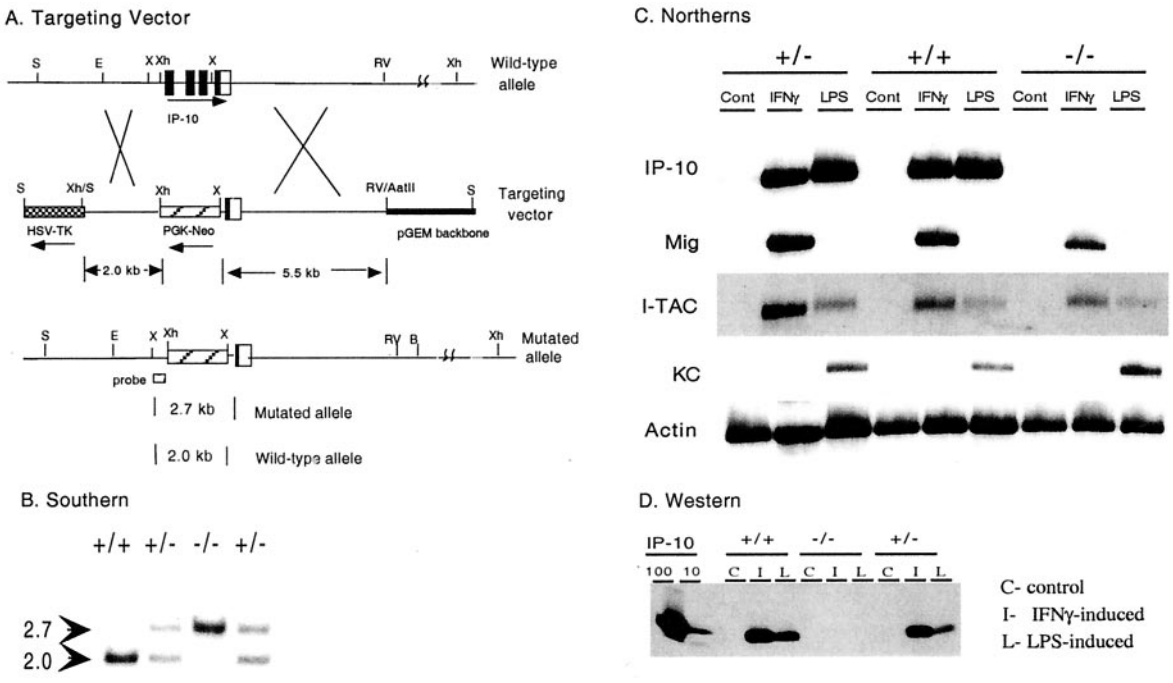

FIGURE 1. Targeted disruption of the murine IP-10 gene. *A*, Wild-type IP-10 allele, targeting vector, and IP-10 deleted allele. IP-10-coding exons 1–3 (■) were deleted and replaced by the neomycin resistance gene driven by the phosphoglycerate kinase promoter (PGK-neo). Negative selection was provided by the thymidine kinase gene driven by the HSV promoter. Relevant restriction endonuclease sites are indicated: B, *Bam*HI; E, *Eco*RI; RV, *Eco*RV; S, *Sal*I; X, *Xba*I; Xh, *Xho*I. *B*, Southern blot analysis of DNA isolated from IP-10 wild-type (+/+), IP-10 heterozygous (+/−), and IP-10 homozygous (−/−) mice for the disrupted IP-10 allele. DNA was digested using *Xba*I and was analyzed by Southern blotting using the probe indicated in *A*. The wild-type allele migrates as a 2-kb hybridizing fragment and the disrupted allele as a 2.7-kb hybridizing band. *C*, Northern blot analysis of chemokine expression. RNA was harvested from bone marrow macrophages isolated from IP-10$^{+/+}$, IP-10$^{+/-}$, and IP-10$^{-/-}$ mice; stimulated with medium control, IFN-γ, or LPS; and analyzed for chemokine expression using cDNA probes specific for IP-10, Mig, I-TAC, KC, and actin as a control for loading. *D*, Supernatants were similarly harvested from stimulated bone marrow macrophages, concentrated, and analyzed for IP-10 protein secretion by Western blot using an affinity-purified anti-murine IP-10 Ab. rIP-10 (100 and 10 ng) was used as a positive control.

stimulated comparable allogeneic responses by BALB/c responder splenocytes (Fig. 2*B*). These data demonstrate that IP-10$^{-/-}$ T cells exhibit an impaired proliferative response to allogeneic stimulation.

Decreased proliferation and IFN-γ secretion to exogenous Ag in IP-10$^{-/-}$ mice

To examine the role of IP-10 in T cell priming, we analyzed the immune response of IP-10$^{+/+}$ and IP-10$^{-/-}$ mice following primary immunization with a model Ag. IP-10$^{+/+}$ and IP-10$^{-/-}$ mice were immunized with 100 μg OVA in CFA. Seven days later, mesenteric lymph nodes were harvested, and cells were restimulated in vitro with OVA for 48 h. The Ag-specific proliferative response of IP-10$^{-/-}$ mice was significantly reduced (~65% reduced; $p = 0.027$; Fig. 3*A*) compared with that of IP-10$^{+/+}$ mice. Another characteristic of T cell activation is cytokine production following Ag stimulation. Secretion of IFN-γ, a potent Th1-type cytokine, was reduced by ~60% in OVA-stimulated IP-10$^{-/-}$ lymphocyte cultures compared with IP-10$^{+/+}$ cultures ($p = 0.021$; Fig. 3*B*). Levels of IL-4 were not detectable by ELISA in either group, and levels of IL-5 were not significantly different (data not shown). To ensure that the differences we observed were not the result of a difference in the kinetics of T cell activation in IP-10$^{-/-}$ mice, we immunized IP-10$^{-/-}$ and IP-10$^{+/+}$ mice with OVA, harvested mesenteric lymph nodes on days 3, 7, 10, and 14 days postimmunization, and measured proliferation and IFN-γ secretion after in vitro restimulation with OVA. IP-10$^{-/-}$ mice exhibited the same kinetics of Ag-induced proliferation and peak IFN-γ secretion as IP-10$^{+/+}$ mice, although at lower levels (data not shown).

IFN-γ has been demonstrated to induce Ig heavy chain class switching to IgG2a, while it inhibits class switching to IgG1 and IgE induced by IL-4 (50). Because IFN-γ secretion in response to Ag stimulation was impaired in IP-10$^{-/-}$ mice, we examined the levels of serum IgG2a, IgG2b, and IgG1 on day 7 post-OVA immunization using an OVA-specific Ig isotype ELISA. The levels of OVA-specific IgG2a were significantly reduced (~56% reduced; $p < 0.027$; Fig. 3*C*) in serum from IP-10$^{-/-}$ mice compared with that from IP-10$^{+/+}$ mice.

IP-10$^{-/-}$ mice exhibit a reduced contact hypersensitivity response

To elucidate the role of IP-10 in the development of a Th1-mediated immune response in vivo where IP-10 has been shown to be up-regulated, we used an experimental model of contact hypersensitivity (51). Results from several studies support a role for both CD4$^+$ and CD8$^+$ T cells and IFN-γ as the effectors of this response (52, 53). During the contact hypersensitivity response, chemokines, including IP-10 and monocyte chemoattractant protein-1 (MCP-1, CCL2), are expressed and thought to mediate the influx of leukocytes into the skin (51, 54, 55). Mice were sensitized with DNFB and 7 days later were challenged by hapten application on the inner and outer skin of the ear. IP-10$^{-/-}$ mice exhibited a small (~28%), yet statistically significant, reduction in ear swelling compared with IP-10$^{+/+}$ mice ($p = 0.01$; Fig. 4). Unsensitized IP-10$^{-/-}$ and IP-10$^{+/+}$ mice challenged with DNFB in acetone demonstrated a comparable modest increase in ear swelling, indicating that IP-10 does not play a role in the acute irritant response (data not shown). Histopathologic analysis of ear tissue revealed

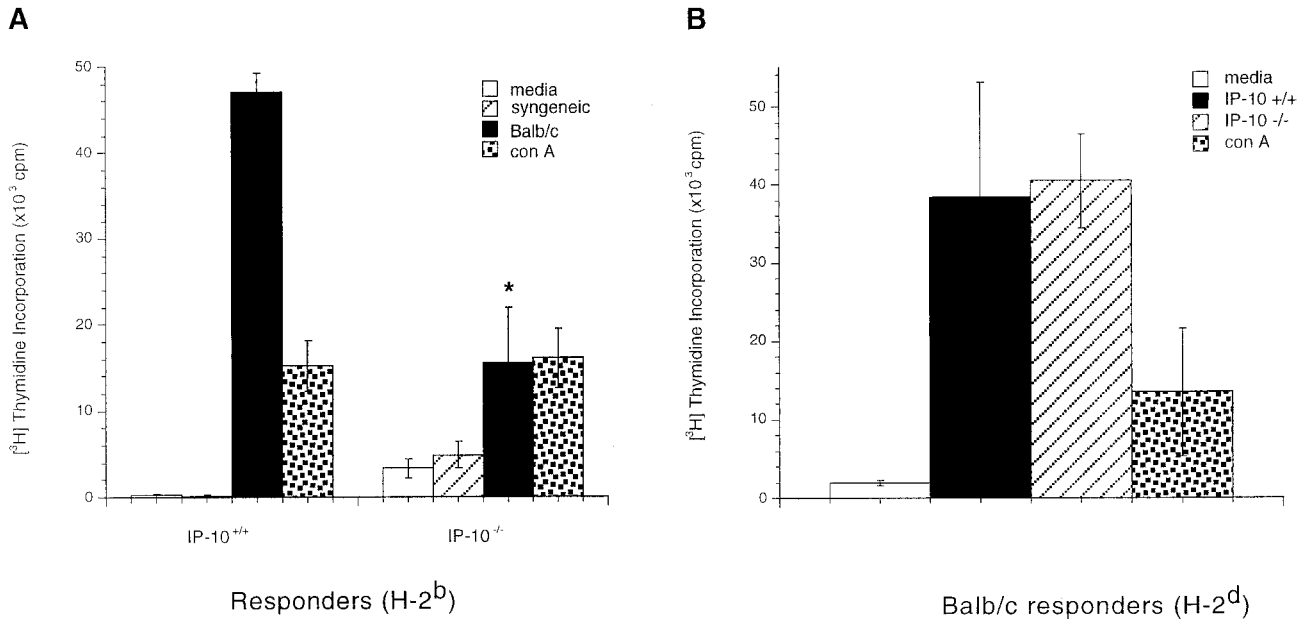

FIGURE 2. IP-10$^{-/-}$ mice exhibit an impaired allogeneic response. Splenocytes from naive IP-10$^{+/+}$ and IP-10$^{-/-}$ 129Sv/J mice (H-2^b) or BALB/c (H-2^d) mice were cocultured in vitro with mitomycin C-treated syngeneic or allogeneic splenocytes or 10 μg/ml Con A. Proliferation of IP-10$^{+/+}$ and IP-10$^{-/-}$ splenocytes in response to BALB/c allogeneic stimulation is shown in *A*, and proliferation of BALB/c splenocytes in response to stimulation with IP-10$^{+/+}$ and IP-10$^{-/-}$ mitomycin C-treated allogeneic splenocytes is shown in *B*. Proliferation was determined by incorporation of [^{3}H]thymidine. *, Significantly decreased proliferation compared with the IP-10$^{+/+}$ response ($p = 0.021$). Data are presented as the mean ± SD derived from triplicate determinations using three animals per genotype. Results from one representative experiment of three performed are shown.

significant edema and inflammatory leukocyte infiltrates in IP-10$^{+/+}$ mice, which were reduced in ear tissue from IP-10$^{-/-}$ mice (Fig. 4*A*). To more directly determine the effects of IP-10 depletion on T cell function in this model, lymphocytes from draining cervical lymph nodes excised at 24 h postchallenge were stimulated in vitro with DNBS, a water-soluble analog of DNFB. Ag-specific proliferation was reduced by ~54% in IP-10$^{-/-}$ mice compared with IP-10$^{+/+}$ mice ($p = 0.032$; Fig. 4*C*). This decrease in Ag-induced proliferation of lymphocytes may be the result of fewer Ag-specific T cells recruited into the draining lymph nodes, an impaired T cell proliferative response in IP-10$^{-/-}$ mice, or a combination of both.

IP-10$^{-/-}$ mice exhibit impaired immunity to MHV infection

We also examined the role of IP-10 in the host response to a viral pathogen that requires T cell-mediated, organ-specific immunity. Previous studies have shown that IP-10 is expressed by astrocytes during acute encephalomyelitis in mice infected with the neurotropic coronavirus MHV, and the majority of T lymphocytes that infiltrate the CNS express CXCR3 (38). To determine the role of IP-10 in viral clearance from the CNS, both IP-10$^{+/+}$ and IP-10$^{-/-}$ mice were infected with MHV, and viral titers were examined at 7 and 12 days p.i. At 7 days p.i., both IP-10$^{+/+}$ and IP-10$^{-/-}$ mice showed comparable levels of virus. However, by day

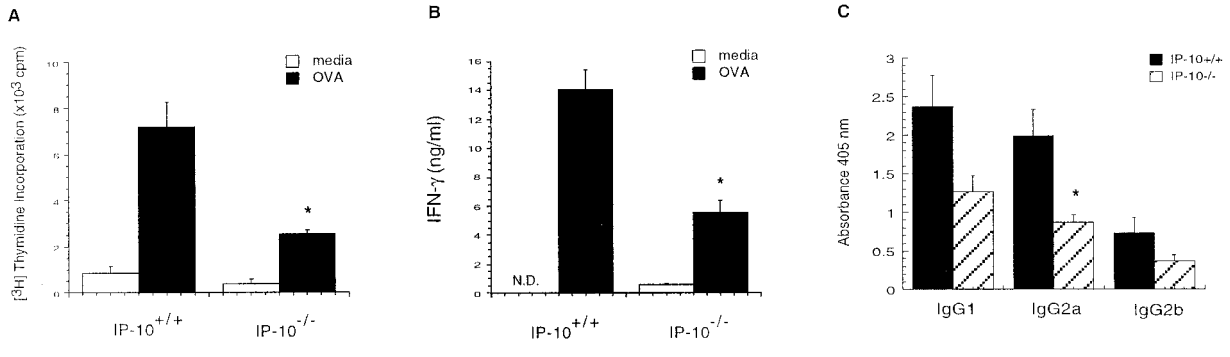

FIGURE 3. Diminished T cell response to OVA in IP-10$^{-/-}$ mice. Mesenteric lymph nodes were harvested from IP-10$^{+/+}$ and IP-10$^{-/-}$ mice immunized i.p. 7 days previously with OVA in CFA. Single-cell suspensions were stimulated in vitro with OVA or medium control for 48 h. Proliferation was determined by incorporation of [^{3}H]thymidine, and IFN-γ levels were determined by ELISA. *, Significantly decreased proliferation ($p = 0.027$) and IFN-γ secretion ($p = 0.021$) compared with IP-10$^{+/+}$ mice. These data are derived from triplicate determinations using three mice per group in two independently performed experiments. N.D., Nondetectable. *C*, Serum was collected from three to five animals per genotype 7 days postimmunization with OVA, diluted 1/100, and assayed for the indicated Ig isotypes by OVA-specific ELISA. OVA-specific Ig levels in preimmune sera were not significantly above background and are not shown. Results from one representative experiment of three performed are shown. *, Significantly reduced levels compared with IP-10$^{+/+}$ mice ($p < 0.027$).

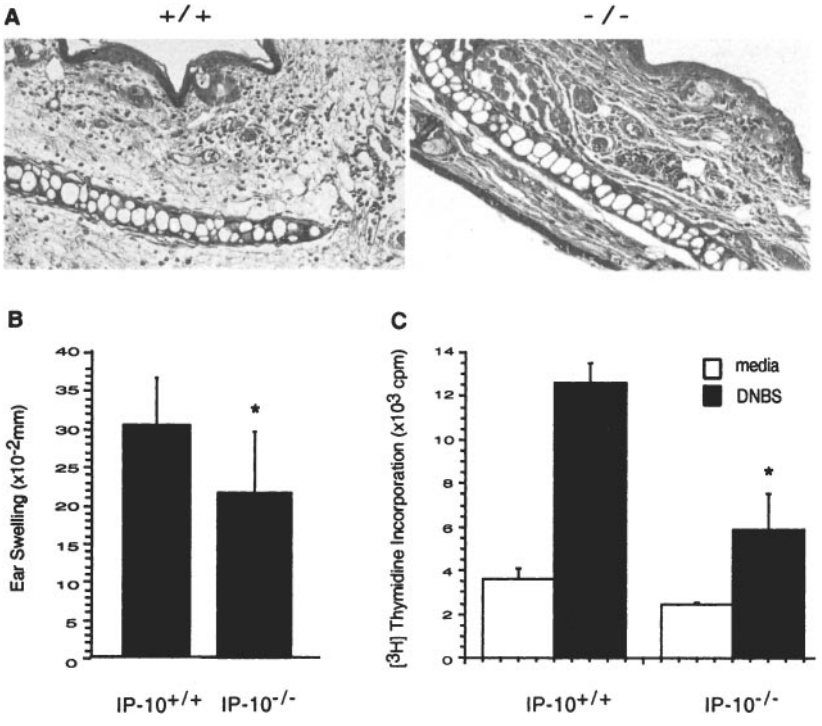

FIGURE 4. The contact hypersensitivity response is reduced in IP-10$^{-/-}$ mice. IP-10$^{+/+}$ and IP-10$^{-/-}$ mice were sensitized epicutaneously on the back with DNFB and 6 days later were challenged on the ear with DNFB. *A*, H&E-stained, formalin-fixed sections of ears from DNFB-sensitized and challenged mice demonstrate increased edema and mononuclear cell infiltrate in ears from IP-10$^{+/+}$ mice compared with IP-10$^{-/-}$ mice. Original magnification, ×20. *B*, Ear swelling was measured at 24 h post-DNFB challenge (*, $p = 0.01$; $n = 8$ experiments, 37 mice per genotype). *C*, Cervical lymph nodes were harvested from mice 24 h post-DNFB challenge on the ear. Single-cell suspensions of lymph node cells were stimulated in vitro with DNBS for 48 h, and proliferation was determined by incorporation of [^{3}H]thymidine. The results represent five mice per group in two independent experiments (*, $p = 0.032$).

12 p.i., IP-10$^{-/-}$ mice displayed significantly higher titers of virus (3.13 ± 0.21 $\log_{10}$ PFU/g) compared with IP-10$^{+/+}$ mice, which cleared virus below the levels of assay sensitivity (<2 $\log_{10}$ PFU/g; $p < 0.001$; Fig. 5*A*).

Recent studies have shown an important role for both CD4$^+$ and CD8$^+$ T lymphocytes in the clearance of virus following MHV infection of the CNS (46). To examine whether increased viral burden within the CNS of IP-10$^{-/-}$ mice correlated with decreased T lymphocyte infiltration, flow cytometric analysis was performed on days 7 and 12 p.i. IP-10$^{-/-}$ mice showed a significant decrease in both CD4$^+$ and CD8$^+$ T lymphocyte infiltration (~78 and ~75% decreases, respectively; $p < 0.01$) as well as a significant decrease in macrophage infiltration (~43% decrease; $p < 0.05$) compared with IP-10$^{+/+}$ mice at day 7 p.i. (Fig. 5*A*). By day 12 both CD4$^+$ and CD8$^+$ T cell numbers remained significantly lower in brains of IP-10$^{-/-}$ mice compared with IP-10$^{+/+}$ mice. Macrophage numbers on day 12 were reduced in IP-10$^{-/-}$ mice compared with wild-type mice, although not significantly.

One mechanism by which T cells contribute to host defense against MHV infection of the CNS is through the release of IFN-γ (56). To determine whether IFN-γ levels were altered in MHV-infected IP-10$^{-/-}$ mice, cytokine transcript levels within the CNS of IP-10$^{-/-}$ and IP-10$^{+/+}$ mice were evaluated by RT-PCR on day 7 p.i. IP-10$^{-/-}$ mice display a marked decrease in IFN-γ expression compared with IP-10$^{+/+}$ mice (Fig. 5*B*).

The decrease in T lymphocyte infiltration following CNS viral infection of IP-10$^{-/-}$ mice suggested that other chemokines were not adequately compensating for the loss of IP-10 activity. Mig and I-TAC are the two additional CXCR3 chemokine agonists described and are also potent chemoattractants for activated T lymphocytes. However, unlike IP-10, which is inducible by both IFN-αβ as well as IFN-γ, Mig expression is more dependent on IFN-γ (1, 57). The decrease in CNS IFN-γ expression suggested that the expression of Mig and I-TAC may also be affected in MHV-infected IP-10$^{-/-}$ mice. Examination of Mig and I-TAC transcripts at 7 days p.i. using RT-PCR showed a marked decrease in the level of CNS Mig and I-TAC mRNA in IP-10$^{-/-}$ mice compared with IP-10$^{+/+}$ mice (Fig. 5*B*). These data suggest that in the absence of IP-10, Th1 cells are not effectively recruited into the brain, resulting in decreased IFN-γ production and therefore decreased Mig and I-TAC expression.

Decreased numbers of effector CD8 T lymphocytes in the spleen following MHV infection of IP-10$^{-/-}$ mice

The absence of IP-10 activity resulted in inhibition of a protective Th1 response characterized by decreased numbers of infiltrating T cells and IFN-γ expression in the brain. To determine whether IP-10 plays a role in the generation of MHV-specific effector T cells, the CD8$^+$ T cell response to virus in MHV-infected IP-10$^{+/+}$ and IP-10$^{-/-}$ mice was evaluated. Mice from both groups received an i.p. injection of MHV (2×10^5 PFU), spleens were removed at day 8 postinjection, and a single-cell suspension was obtained. The immunodominant epitope of MHV recognized by CD8$^+$ T cells is found on the surface glycoprotein at residues 510–518 (S510–518) (48, 49). Isolated splenocytes from IP-10$^{+/+}$ and IP-10$^{-/-}$ mice were stimulated with the CD8 viral epitope (S510–518) and dual stained for CD8 and IFN-γ. The total numbers of cells found within the spleens of IP-10$^{+/+}$ and IP-10$^{-/-}$ mice were comparable. However, the total number of CD8$^+$ T cells within the spleens of IP-10$^{-/-}$ mice was decreased by ~25% compared with that in IP-10$^{+/+}$ mice (IP-10$^{-/-}$, 4.5×10^6 cells; IP-10$^{+/+}$, 6×10^6 cells). In addition, IP-10$^{-/-}$ mice had a decrease (~40%) in the percentage of CD8$^+$ T lymphocytes responding to viral peptide S510–518 compared with IP-10$^{+/+}$ mice (Fig. 6*A*). Furthermore, such analysis revealed an ~2-fold decrease in total numbers of activated CD8$^+$ T lymphocytes present within the spleen of immunized IP-10$^{-/-}$ mice compared with IP-10$^{+/+}$ (Fig. 6*B*). Collectively, these data suggest that the generation and/or effector activity of CD8$^+$ T lymphocytes were affected by the absence of IP-10 activity.

Reduced demyelination in MHV-infected IP-10$^{-/-}$ mice

Effector T lymphocytes and macrophages are important in driving MHV-induced demyelination (46). Further, a recent study by Liu

A Decreased Viral Clearance and Recruitment of T lymphocytes in IP-10$^{-/-}$ mice

Mouse	PID	Log_{10} PFU/g	Cell recovery	CD4$^+$	CD8$^+$	F4/80$^+$
IP-10$^{+/+}$	7	4.14 ± 1.05	5.2x10^6	9.8 ± 2.0[a]	8.1 ± 1.2	13 ± 1.4
IP-10$^{-/-}$	7	4.35 ± 0.07	4.2x10^6	2.1 ± 0.4[b]	2.0 ± 0.8[b]	7.4 ± 1.3[c]
IP-10$^{+/+}$	12	<2	4.3x10^6	5.6 ± 0.3	4.0 ± 0.7	13 ± 25
IP-10$^{-/-}$	12	3.13±0.21[a]	3.3x10^6	2.7 ± 0.03[b]	2.6 ± 0.2[c]	7.3 ± 1.3

[a] data presented as average total cells x10^5 ± SEM
[b] p<0.001 when compared to IP-10$^{+/+}$ mice
[c] p<0.05 when compared to IP-10$^{+/+}$ mice

B RT-PCR Analysis

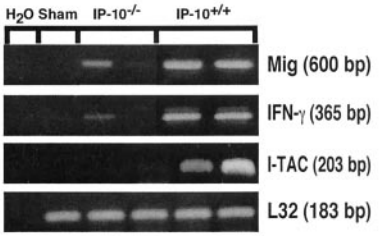

FIGURE 5. Impaired host response to MHV infection in IP-10$^{-/-}$ mice. *A*, Delayed viral clearance from the brain and decreased recruitment of T lymphocytes into the brain in MHV-infected IP-10$^{-/-}$ mice. Brains of infected mice were removed at 7 and 12 days p.i., and one-half was used for a plaque assay to determine viral burden. Single-cell suspensions were obtained, and cell recovery was calculated as the average yield from Percoll gradients. Cellular infiltrate was immunophenotyped by flow cytometry and is presented as the total number of CD4$^+$, CD8$^+$, and F4/80$^+$ cells [(percentage of positive cells within the gated population) × (total number of cells recovered)]. Data represent two to five mice per group examined in two independent experiments. *B*, RT-PCR analysis of chemokine and cytokine mRNA. RT-PCR analysis of Mig, I-TAC, and IFN-γ expression was performed in brains of mice at 7 days p.i. using primers for Mig, I-TAC, IFN-γ, or L32 ribosomal control. Sham controls were mice that received an i.c. injection of 30 μl sterile saline.

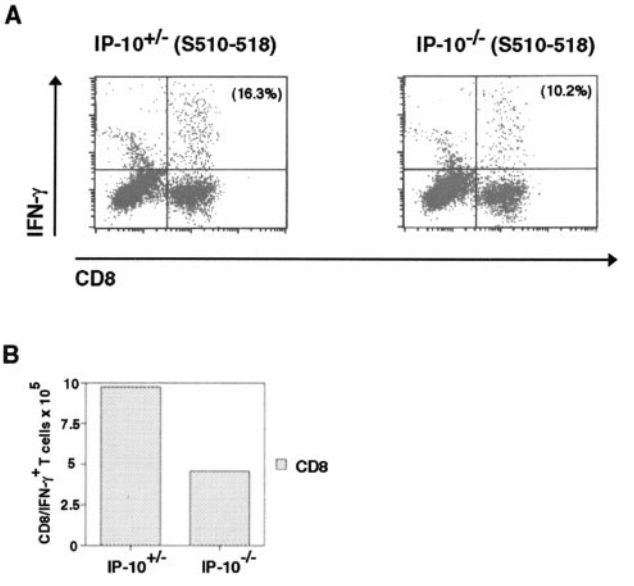

FIGURE 6. Decreased viral-specific CD8$^+$ effector T cells in IP-10$^{-/-}$ mouse cells. Analysis of MHV-specific CD8$^+$ T cells in IP-10$^{+/+}$ and IP-10$^{-/-}$ mice. Splenocytes were harvested from spleens 8 days after immunization with MHV, and the CD8 response to virus was determined. Cells were stained for CD8, and IFN-γ expression was evaluated following stimulation with the CD8 epitope S510–518. *A*, The percentage of dual-positive cells in immunized mice is indicated in the parentheses in the *upper right quadrants*. IP-10$^{-/-}$ mice display an ~40% decrease in the percentage of activated CD8$^+$ T cells (as measured by IFN-γ secretion) compared with IP-10$^{+/+}$ mice. *B*, Total numbers of dual-positive cells responding to the S510–518 epitope. Correlating with the decrease in percentage of activated CD8$^+$ T cells is a marked decrease in the numbers of virus-specific CD8$^+$ T cells within the spleens of IP-10$^{-/-}$ mice compared with IP-10$^{+/+}$mice.

et al. (39) showed that Ab-mediated neutralization of IP-10 during established MHV-induced demyelination resulted in diminished clinical and histological disease that correlated with decreased CD4$^+$ T cell and macrophage infiltration within the CNS. Taken together, these data suggest that demyelination may be altered within the CNS of IP-10$^{-/-}$ mice. To address this possibility, demyelination was assessed within LFB-stained spinal cords taken from IP-10$^{-/-}$ and IP-10$^{+/+}$ mice infected with MHV at 12 days p.i. As shown in Fig. 7, mice lacking IP-10 displayed significantly reduced ($p < 0.005$) levels of demyelination compared with wild-type mice, supporting Ab neutralization studies that indicated a prominent role for this chemokine in contributing to MHV-induced demyelination.

Discussion

In this study mice deficient in IP-10 were generated and described. IP-10$^{-/-}$ mice had no discernable immunologic abnormalities at baseline, but did exhibit impaired T cell immune responses when challenged in vivo. IP-10$^{-/-}$ mice had an impaired proliferative response to allogeneic stimulation in the mixed lymphocyte response. Following primary immunization with OVA, IP-10$^{-/-}$ mice had a reduced recall response, characterized by decreased Ag-induced proliferation and reduced IFN-γ secretion, supporting a role for IP-10 in T cell priming in vivo. IP-10$^{-/-}$ mice also exhibited an impaired contact hypersensitivity response, characterized by decreased ear swelling and reduced inflammatory cell infiltrates. In addition, lymphocytes from draining lymph nodes of sensitized and challenged IP-10$^{-/-}$ mice had a decreased proliferative response to Ag restimulation in vitro. Lastly, IP-10$^{-/-}$ mice infected with a neurotropic MHV had an impaired ability to control viral replication in the brain. This was associated with decreased recruitment of CD4$^+$ and CD8$^+$ lymphocytes into the brain; reduced levels of IFN-γ, Mig, and I-TAC in the brain; and impaired generation of viral-specific CD8$^+$ T cells. Thus, IP-10 appears to play a role in both the generation of effector T cells and their delivery to sites of tissue inflammation.

Increasing data support the concept that IP-10 plays an important role in attracting effector T cells into sites of Th1-type inflammation. IP-10 is highly expressed in the tissue in Th1 inflammation, and CXCR3$^+$ T cells are found to be highly enriched juxtaposed to IP-10 at these inflammatory sites. Our study demonstrated that IP-10$^{-/-}$ mice have decreased inflammatory cell recruitment into the skin in a contact hypersensitivity response and decreased effector T cell recruitment into the CNS in a murine model of MHV infection resulting in reduced demyelination These data are consistent with Ab neutralization studies, which have revealed a role for IP-10 in effector T cell trafficking into organs infected with the intracellular parasite *T. gondii* (34) and into the CNS in a murine model of EAE (37) and MHV infection (38). Furthermore, recent studies with the IP-10$^{-/-}$ mice we describe here and with CXCR3$^{-/-}$ mice demonstrated a role for donor-derived IP-10 and host-derived CXCR3 in the recruitment of NK cells and effector T cells into murine cardiac allografts delaying rejection (41, 58). Thus, data from Ab neutralization studies and gene-targeted mice indicate that IP-10 plays an important nonredundant role in the recruitment of effector T cells into tissue sites in certain inflammatory responses.

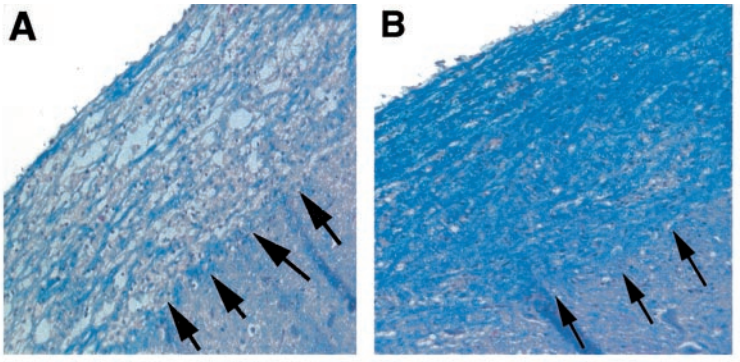

FIGURE 7. Demyelination is reduced in IP-10$^{-/-}$ mice infected with MHV. LFB-stained spinal cords taken from either IP-10$^{+/+}$ (*A*) or IP-10$^{-/-}$ (*B*) mice at 12 days p.i. Note the pronounced inflammation and destruction of myelin sheath (arrows) within IP-10$^{+/+}$ mice in contrast to IP-10$^{-/-}$ mice, which display a compact myelin sheath. *C*, Demyelination score for spinal cords isolated from groups of IP-10$^{+/+}$ and IP-10$^{-/-}$ mice stained with LFB at day 12 p.i.

C

Mouse Genotype	days post infection	n	Demyelination score
IP-10 $^{+/+}$	12	7	2.8 ± 0.22 [a]
IP-10 $^{-/-}$	12	6	1.3 ± 0.30 [b]

[a] data presented as mean ± SEM. Data are representative of two separate experiments.
[b] $p<0.005$ when compared to IP-10$^{+/+}$ mice.

In addition to a role in effector T cell trafficking, the data presented here demonstrate that IP-10 participates in the generation of effector T cells in vivo. IP-10$^{-/-}$ mice infected with MHV had fewer Ag-specific IFN-γ-secreting CD8 cells in the spleen. In addition, following immunization with a model Ag (OVA) or immunization and challenge with a hapten (DNFB), T cells isolated from draining lymph nodes had decreased Ag-induced proliferative response and IFN-γ secretion. Data from mAb neutralization studies support this concept. In an IL-12 gene therapy model, mAb neutralization of IP-10 only during the immunization phase markedly impaired the generation of tumor-specific effector T cells and subsequent tumor protective immunity (43). Similarly, neutralization of IP-10 following acute *T. gondii* infection impaired the generation of Ag-specific T cells found in the spleen (34). Thus, studies using Ab neutralization and genetically deficient mice have revealed an unexpected role for IP-10 and its receptor CXCR3 in the generation of Ag-specific effector T cells.

The mechanism(s) by which IP-10 influences the generation of effector T cells has not been established, but published data point in two directions: dendritic cell trafficking and costimulation of T cells. Chemokines guide Ag-loaded dendritic cells from the tissue and naive T cells from the blood into close contact in the lymph node to generate an immune response. SLC (CCL22) and ELC (CCL19) are chemokines that are constitutively expressed in lymphoid tissue and along with their receptor, CCR7, play important roles in this process (59). However, it has become clear that other chemokines, more commonly thought of as inducible chemokines, such as IP-10 and MCP-1, are also constitutively expressed in lymphoid tissue (2, 60) and may also contribute to dendritic cell trafficking. For example, MCP-1 has been shown to play a role in guiding dendritic cells from the periphery into lymph nodes following Ag challenge (61, 62). IP-10 could play a similar role in vivo. In this regard, it is interesting to note that CXCR3 is expressed on plasmacytoid dendritic cells generated following an inflammatory stimulus (22, 63) as well as myeloid dendritic cells found in normal lymph nodes, which have been shown to chemotax in response to IP-10 (23). It has been proposed that constitutive IP-10 expressed in lymph node and spleen attracts Ag-loaded dendritic cells into lymphoid tissue, facilitating dendritic cell and naive T cell interactions, which generate effector T cells (64).

In addition to regulating leukocyte trafficking, chemokines have been suggested to play a role in leukocyte activation. It is well established that chemokines can induce granule release from monocytes, neutrophils, eosinophils, and basophils. Data are also accumulating that chemokines can participate in lymphocyte activation. For example, SDF-1 (CXCL12) is a well-characterized B cell growth factor (65–67) and has recently been described as a costimulator of T cell activation (68). Our finding that IP-10$^{-/-}$ mice exhibited a decreased allogeneic response is consistent with data reported for the CXCR3$^{-/-}$ mice, which exhibited decreased MLR of similar magnitude (58). These data together with published data demonstrating that activated T cells release IP-10 (2) and that the expression of CXCR3 is increased on T cells following activation in the MLR (69) suggest that IP-10 may costimulate T cell activation in an autocrine loop. However, the contribution of IP-10 to T cell activation can be overcome, because we have previously found that host-derived IP-10 is not essential for the generation of an immune response capable of inducing rejection following allogenic cardiac transplantation (41). The mechanism(s) by which IP-10 may activate T cells is currently unknown. However, a recent report provides evidence that the extracellular signal-regulated kinase pathway may be involved. IP-10 activation of CXCR3 on vascular pericytes was demonstrated to induce proliferation of these cells, and pharmacologic inhibition of the extracellular signal-regulated kinase pathway reduced this response (70).

In summary, we found that IP-10$^{-/-}$ mice exhibit decreased T cell proliferative responses to allogeneic stimulation and decreased T cell priming following primary immunization with exogenous Ag. In vivo studies demonstrated that IP-10$^{-/-}$ mice have a reduced contact hypersensitivity response and impaired host immune response to MHV. In both models this was associated with decreased recruitment of T cells into tissues as well as an impairment in the generation of Ag-specific effector T cells in the periphery. Thus, the generation of IP-10$^{-/-}$ mice has revealed a role for

IP-10 in both the generation of effector T cells and their delivery to sites of tissue inflammation.

Acknowledgments

We thank Dr. En Li for helpful advice with constructing the targeting vector, ES cell electroporations, and blastocyst injections, and we thank Dr. Andrew M. Tager for critical review of this manuscript.

References

1. Luster, A. D., J. C. Unkeless, and J. V. Ravetch. 1985. γ-Interferon transcriptionally regulates an early-response gene containing homology to platelet proteins. *Nature 315:672.*
2. Gattass, C. R., L. B. King, A. D. Luster, and J. D. Ashwell. 1994. Constitutive expression of IP-10 in lymphoid organs and inducible expression in T cells and thymocytes. *J. Exp. Med. 179:1373.*
3. Luster, A. D., and J. V. Ravetch. 1987. Biochemical characterization of a γ interferon-inducible cytokine (IP-10). *J. Exp. Med. 166:1084.*
4. Vanguri, P., and J. M. Farber. 1990. Identification of CRG-2: an interferon-inducible mRNA predicted to encode a murine monokine. *J. Biol. Chem. 265: 15049.*
5. Ohmori, Y., and T. A. Hamilton. 1990. A macrophage LPS-inducible early gene encodes the murine homologue of IP-10. *Biochem. Biophys. Res. Commun. 168: 1261.*
6. Gottlieb, A. B., A. D. Luster, D. N. Posnett, and D. M. Carter. 1988. Detection of a γ interferon-induced protein IP-10 in psoriatic plaques. *J. Exp. Med. 168: 941.*
7. Flier, J., D. M. Boorsma, P. J. van Beek, C. Nieboer, T. J. Stoof, R. Willemze, and C. P. Tensen. 2001. Differential expression of CXCR3 targeting chemokines CXCL10, CXCL9, and CXCL11 in different types of skin inflammation. *J. Pathol. 194:398.*
8. Sorensen, T. L., M. Tani, J. Jensen, V. Pierce, C. Lucchinetti, V. A. Folcik, S. Qin, J. Rottman, F. Sellebjerg, R. M. Strieter, et al. 1999. Expression of specific chemokines and chemokine receptors in the central nervous system of multiple sclerosis patients. *J. Clin. Invest. 103:807.*
9. Balashov, K., J. Rottman, H. Weiner, and W. Hancock. 1999. $CCR5^+$ and $CXCR3^+$ T cells are increased in multiple sclerosis and their ligands MIP-1 and IP-10 are expressed in demyelinating brain lesions. *Proc. Natl. Acad. Sci. USA 96:6873.*
10. Mach, F., A. Sauty, A. S. Iarossi, G. K. Sukhova, K. Neote, P. Libby, and A. D. Luster. 1999. The interferon-γ inducible CXC chemokines IP-10, Mig, and I-TAC are differentially expressed by human atheroma-associated cells: implications for lymphocyte recruitment in atherogenesis. *J. Clin. Invest. 104:1041.*
11. Patel, D. D., J. P. Zachariah, and L. P. Whichard. 2001. CXCR3 and CCR5 ligands in rheumatoid arthritis synovium. *Clin. Immunol. 98:39.*
12. Melter, M., A. Exeni, M. E. Reinders, J. C. Fang, G. McMahon, P. Ganz, W. W. Hancock, and D. M. Briscoe. 2001. Expression of the chemokine receptor CXCR3 and its ligand IP-10 during human cardiac allograft rejection. *Circulation 104:2558.*
13. Agostini, C., F. Calabrese, F. Rea, M. Facco, A. Tosoni, M. Loy, G. Binotto, M. Valente, L. Trentin, and G. Semenzato. 2001. CXCR3 and its ligand CXCL10 are expressed by inflammatory cells infiltrating lung allografts and mediate chemotaxis of T cells at sites of rejection. *Am. J. Pathol. 158:1703.*
14. Grimm, M. C., and W. F. Doe. 1996. Chemokines in inflammatory bowel disease mucosa: expression of RANTES, macrophage inflammatory protein (MIP)-1α, MIP-1β, and γ-interferon-inducible protein-10 by macrophages, lymphocytes, endothelial cells, and granulomas. *Inflamm. Bowel Dis. 2:88.*
15. Lahrtz, F., L. Piali, D. Nadal, H.-W. Pfister, K.-S. Spanaus, M. Baggiolini, and A. Fontana. 1997. Chemokines in viral meningitis: chemotactic cerebrospinal fluid factors include MCP-1 and IP-10 for monocytes and activate T lymphocytes. *Eur. J. Immunol. 27:2484.*
16. Agostini, C., M. Cassatella, R. Sancetta, R. Zambello, L. Trentin, S. Gasperini, A. Perin, F. Piazza, M. Siviero, M. Facco, et al. 1998. Involvement of the IP-10 chemokine in sarcoid granulomatous reactions. *J. Immunol. 161:6413.*
17. Narumi, S., Y. Tominaga, M. Tamaru, S. Shimai, H. Okumura, K. Nishioji, Y. Itoh, and T. Okanoue. 1997. Expression of IFN-inducible protein-10 in chronic hepatitis. *J. Immunol. 158:5536.*
18. Loetscher, M., B. Gerber, P. Loetscher, S. A. Jones, L. Piali, I. Clark-Lewi, M. Baggiolini, and B. Moser. 1996. Chemokine receptor specific for IP10 and Mig: structure, function, and expression in activated T-lymphocytes. *J. Exp. Med. 184:963.*
19. Loetscher, P., M. Uguccioni, L. Bordoli, M. Baggiolini, B. Moser, C. Chizzolini, and J.-M. Dayer. 1998. CCR5 is characteristic of Th1 lymphocytes. *Nature 391: 344.*
20. Qin, S., J. B. Rottman, P. Myrers, N. Kassam, M. Weinblatt, M. Loetscher, A. E. Koch, B. Moser, and C. R. Mackay. 1998. The chemokine receptors CXCR3 and CCR5 mark subsets of T cells associated with certain inflammatory reactions. *J. Clin. Invest. 101:746.*
21. Butcher, E., and L. Picker. 1996. Lymphocyte homing and homeostasis. *Science 1996 272:60.*
22. Cella, M., D. Jarrossay, F. Facchetti, O. Alebardi, H. Nakajima, A. Lanzavecchia, and M. Colonna. 1999. Plasmacytoid monocytes migrate to inflamed lymph nodes and produce large amounts of type I interferon. *Nat. Med. 5:919.*
23. Garcia-Lopez, M. A., F. Sanchez-Madrid, J. M. Rodriguez-Frade, M. Mellado, A. Acevedo, M. I. Garcia, J. P. Albar, C. Martinez, and M. Marazuela. 2001. CXCR3 chemokine receptor distribution in normal and inflamed tissues: expression on activated lymphocytes, endothelial cells, and dendritic cells. *Lab. Invest. 81:409.*
24. Trentin, L., C. Agostini, M. Facco, F. Piazza, A. Perin, M. Siviero, C. Gurrieri, S. Galvan, F. Adami, R. Zambello, et al. 1999. The chemokine receptor CXCR3 is expressed on malignant B cells and mediates chemotaxis. *J. Clin. Invest. 104: 115.*
25. Jones, D., R. J. Benjamin, A. Shahsafaei, and D. M. Dorfman. 2000. The chemokine receptor CXCR3 is expressed in a subset of B-cell lymphomas and is a marker of B-cell chronic lymphocytic leukemia. *Blood 95:627.*
26. Jinquan, T., C. Jing, H. H. Jacobi, C. M. Reimert, A. Millner, S. Quan, J. B. Hansen, S. Dissing, H. J. Malling, P. S. Skov, et al. 2000. CXCR3 expression and activation of eosinophils: role of IFN-γ-inducible protein-10 and monokine induced by IFN-γ. *J. Immunol. 165:1548.*
27. Romagnani, P., F. Annunziato, L. Lasagni, E. Lazzeri, C. Beltrame, M. Francalanci, M. Uguccioni, G. Galli, L. Cosmi, L. Maurenzig, et al. 2001. Cell cycle-dependent expression of CXC chemokine receptor 3 by endothelial cells mediates angiostatic activity. *J. Clin. Invest. 107:53.*
28. Salcedo, R., J. H. Resau, D. Halverson, E. A. Hudson, M. Dambach, D. Powell, K. Wasserman, and J. J. Oppenheim. 2000. Differential expression and responsiveness of chemokine receptors (CXCR1–3) by human microvascular endothelial cells and umbilical vein endothelial cells. *FASEB J. 14:2055.*
29. Romagnani, P., F. Annunziato, E. Lazzeri, L. Cosmi, C. Beltrame, L. Lasagni, G. Galli, M. Francalanci, R. Manetti, F. Marra, et al. 2001. Interferon-inducible protein 10, monokine induced by interferon γ, and interferon-inducible T-cell α chemoattractant are produced by thymic epithelial cells and attract T-cell receptor (TCR) $\alpha\beta^+CD8^+$ single-positive T cells, $TCR\gamma\delta^+$ T cells, and natural killer-type cells in human thymus. *Blood 97:601.*
30. Jinquan, T., S. Quan, H. H. Jacobi, C. Jing, A. Millner, B. Jensen, H. O. Madsen, L. P. Ryder, A. Svejgaard, H. J. Malling, et al. 2000. CXC chemokine receptor 3 expression on $CD34^+$ hematopoietic progenitors from human cord blood induced by granulocyte-macrophage colony-stimulating factor: chemotaxis and adhesion induced by its ligands, interferon γ-inducible protein 10 and monokine induced by interferon γ. *Blood 96:1230.*
31. Farber, J. M. 1993. HuMig: a new human member of the chemokine family of cytokines. *Biochim. Biophys. Acta 192:223.*
32. Cole, K. E., C. A. Strick, T. J. Paradis, K. T. Ogborne, M. Loetscher, R. P. Gladue, W. Lin, J. G. Boyd, B. Moser, D. E. Wood, et al. 1998. Interferon-inducible T cell alpha chemoattractant (I-TAC): a novel non-ELR CXC chemokine with potent activity on activated T cells through selective high affinity binding to CXCR3. *J. Exp. Med. 187:2009.*
33. Widney, D. P., Y. R. Xia, A. J. Lusis, and J. B. Smith. 2000. The murine chemokine CXCL11 (IFN-inducible T cell α chemoattractant) is an IFN-γ- and lipopolysaccharide-inducible glucocorticoid-attenuated response gene expressed in lung and other tissues during endotoxemia. *J. Immunol. 164:6322.*
34. Khan, I., J. A. MacLean, F. Lee, L. Casciotti, E. DeHaan, J. Schwartzman, and A. D. Luster. 2000. The IP-10 chemokine is critical for effector T cell trafficking and host survival in *Toxoplasma gondii* infection. *Immunity 12:483.*
35. Amichay, D., R. T. Gazzinelli, G. Karupiah, T. R. Moench, A. Sher, and J. M. Farber. 1996. Genes for chemokines MuMig and Crg-2 are induced in protozoan and viral infections in response to IFN-γ with patterns of tissue expression that suggest nonredundant roles in vivo. *J. Immunol. 157:4511.*
36. Goebeler, M., A. Toksoy, U. Spandau, E. Engelhardt, E. B. Brocker, and R. Gillitzer. 1998. The CXC chemokine Mig is highly expressed in the papillae of psoriatic lesions. *J. Pathol. 184:89.*
37. Fife, B. T., K. J. Kennedy, M. C. Paniagua, N. W. Lukacs, S. L. Kunkel, A. D. Luster, and W. J. Karpus. 2001. CXCL10 (IFN-γ-inducible protein-10) control of encephalitogenic $CD4^+$ T cell accumulation in the central nervous system during experimental autoimmune encephalomyelitis. *J. Immunol. 166: 7617.*
38. Liu, M. T., B. P. Chen, P. Oertel, M. J. Buchmeier, D. Armstrong, T. A. Hamilton, and T. E. Lane. 2000. The T cell chemoattractant IFN-inducible protein 10 is essential in host defense against viral-induced neurologic disease. *J. Immunol. 165:2327.*
39. Liu, M. T., H. S. Keirstead, and T. E. Lane. 2001. Neutralization of the chemokine CXCL10 reduces inflammatory cell invasion and demyelination and improves neurological function in a viral model of multiple sclerosis. *J. Immunol. 167:4091.*
40. Koga, S., M. B. Auerbach, T. M. Engeman, A. C. Novick, H. Toma, and R. L. Fairchild. 1999. T cell infiltration into class II MHC-disparate allografts and acute rejection is dependent on the IFN-γ-induced chemokine Mig. *J. Immunol. 163:4878.*
41. Hancock, W. W., W. Gao, V. Csizmadia, K. Faia, N. Shemmeri, and A. D. Luster. 2001. Donor-derived IP-10 initiates development of acute allograft rejection. *J. Exp. Med. 193:975.*
42. Gangur, V., F. E. R. Simons, and K. T. Hayglass. 1998. Human IP-10 selectively promotes dominance of polyclonally activated and environmental antigen-driven IFNγ over IL-4 responses. *FASEB J. 12:705.*
43. Pertl, U., A. D. Luster, N. M. Varki, D. Homann, G. Gaedicke, R. A. Reisfeld, and H. N. Lode. 2001. IFN-γ-inducible protein-10 is essential for the generation of a protective tumor-specific CD8 T cell response induced by single-chain IL-12 gene therapy. *J. Immunol. 166:6944.*
44. Ohmori, Y., and T. A. Hamilton. 1993. Cooperative interaction between interferon (IFN) stimulus response element and κB sequence motifs controls IFNγ- and lipopolysaccharide-stimulated transcription from the murine IP-10 promoter. *J. Biol. Chem. 268:6677.*

45. Luster, A. D., S. Greenberg, and P. Leder. 1995. The IP-10 chemokine binds to a specific cell surface heparan sulfate site shared with platelet factor 4 and inhibits endothelial cell proliferation. *J. Exp. Med. 182:219.*
46. Lane, T. E., M. T. Liu, B. P. Chen, V. C. Asensio, R. M. Samawi, A. D. Paoletti, I. L. Campbell, S. L. Kunkel, H. S. Fox, and M. J. Buchmeier. 2000. A central role for CD4$^+$ T cells and RANTES in virus-induced central nervous system inflammation and demyelination. *J. Virol. 74:1415.*
47. Wu, G. F., A. A. Dandekar, L. Pewe, and S. Perlman. 2000. CD4 and CD8 T cells have redundant but not identical roles in virus-induced demyelination. *J. Immunol. 165:2278.*
48. Castro, R. F., and S. Perlman. 1995. CD8$^+$ T-cell epitopes within the surface glycoprotein of a neurotropic coronavirus and correlation with pathogenicity. *J. Virol. 69:8127.*
49. Bergmann, C. C., Q. Yao, M. Lin, and S. A. Stohlman. 1996. The JHM strain of mouse hepatitis virus induces a spike protein-specific Db-restricted cytotoxic T cell response. *J. Gen. Virol. 77:315.*
50. Coffman, R. L., D. A. Lebman, and P. Rothman. 1993. Mechanism and regulation of immunoglobulin isotype switching. *Adv. Immunol. 54:229.*
51. Gautam, S., J. Battisto, J. A. Major, D. Armstrong, M. Stoler, and T. A. Hamilton. 1994. Chemokine expression in trinitrochlorobenzene-mediated contact hypersensitivity. *J. Leukocyte Biol. 55:452.*
52. Gocinski, B. L., and R. E. Tigelaar. 1990. Roles of CD4$^+$ and CD8$^+$ T cells in murine contact sensitivity revealed by in vivo monoclonal antibody depletion. *J. Immunol. 144:4121.*
53. Lu, B., C. Ebensperger, Z. Dembic, Y. Wang, M. Kvatyuk, T. Lu, R. L. Coffman, S. Pestka, and P. B. Rothman. 1998. Targeted disruption of the interferon-γ receptor 2 gene results in severe immune defects in mice. *Proc. Natl. Acad. Sci. USA 95:8233.*
54. Abe, M., T. Kondo, H. Xu, and R. L. Fairchild. 1996. Interferon-γ inducible protein (IP-10) expression is mediated by CD8$^+$ T cells and is regulated by CD4$^+$ T cells during the elicitation of contact hypersensitivity. *J. Invest. Dermatol. 107:360.*
55. Yuan, Y. S., J. A. Major, and J. R. Battisto. 1996. Regulation of chemokine gene expression by contact hypersensitivity and by oral tolerance. *Ann. NY Acad. Sci. 778:434.*
56. Parra, B., D. R. Hinton, N. W. Marten, C. C. Bergmann, M. T. Lin, C. S. Yang, and S. A. Stohlman. 1999. IFN-γ is required for viral clearance from central nervous system oligodendroglia. *J. Immunol. 162:1641.*
57. Farber, J. M. 1997. Mig and IP-10: CXC chemokines that target lymphocytes. *J. Leukocyte Biol. 61:246.*
58. Hancock, W. W., B. Lu, W. Gao, V. Csizmadia, K. Faia, J. A. King, S. T. Smiley, M. Ling, N. P. Gerard, and C. G. Gerard. 2000. Requirement of the chemokine receptor CXCR3 for acute allograft rejection. *J. Exp. Med. 192:1515.*
59. Cyster, J. G. 1999. Chemokines and cell migration in secondary lymphoid organs. *Science 286:2098.*
60. Gu, L., S. Tseng, R. M. Horner, C. Tam, M. Loda, and B. J. Rollins. 2000. Control of TH2 polarization by the chemokine monocyte chemoattractant protein-1. *Nature 404:407.*
61. Peters, W., H. M. Scott, H. F. Chambers, J. L. Flynn, I. F. Charo, and J. D. Ernst. 2001. Chemokine receptor 2 serves an early and essential role in resistance to *Mycobacterium tuberculosis*. *Proc. Natl. Acad. Sci. USA 98:7958.*
62. Sato, N., S. K. Ahuja, M. Quinones, V. Kostecki, R. L. Reddick, P. C. Melby, W. A. Kuziel, and S. S. Ahuja. 2000. CC chemokine receptor (CCR)2 is required for Langerhans cell migration and localization of T helper cell type 1 (Th1)-inducing dendritic cells: absence of CCR2 shifts the *Leishmania major*-resistant phenotype to a susceptible state dominated by Th2 cytokines, β cell outgrowth, and sustained neutrophilic inflammation. *J. Exp. Med. 192:205.*
63. Penna, G., S. Sozzani, and L. Adorini. 2001. Cutting edge: selective usage of chemokine receptors by plasmacytoid dendritic cells. *J. Immunol. 167:1862.*
64. Patterson, S. 2000. Flexibility and cooperation among dendritic cells. *Nat. Immunol. 1:273.*
65. Nagasawa, T., S. Hirota, K. Tachibana, N. Takakura, S. Nishikawa, Y. Kitamura, N. Yoshida, H. Kikutani, and T. Kishimoto. 1996. Defects of B-cell lymphopoiesis and bone-marrow myelopoiesis in mice lacking the CXC chemokine PBSF/SDF-1. *Nature 382:635.*
66. Nagasawa, T., H. Kikutani, and T. Kishimoto. 1994. Molecular cloning and structure of a pre-B-cell growth-stimulating factor. *Proc. Natl. Acad. Sci. USA 91:2305.*
67. Egawa, T., K. Kawabata, H. Kawamoto, K. Amada, R. Okamoto, N. Fujii, T. Kishimoto, Y. Katsura, and T. Nagasawa. 2001. The earliest stages of B cell development require a chemokine stromal cell-derived factor/pre-B cell growth-stimulating factor. *Immunity 15:323.*
68. Nanki, T., and P. E. Lipsky. 2000. Cutting edge: stromal cell-derived factor-1 is a costimulator for CD4$^+$ T cell activation. *J. Immunol. 164:5010.*
69. Ebert, L. M., and S. R. McColl. 2001. Coregulation of CXC chemokine receptor and CD4 expression on T lymphocytes during allogeneic activation. *J. Immunol. 166:4870.*
70. Bonacchi, A., P. Romagnani, R. G. Romanelli, E. Efsen, F. Annunziato, L. Lasagni, M. Francalanci, M. Serio, G. Laffi, M. Pinzani, et al. 2001. Signal transduction by the chemokine receptor CXCR3: activation of Ras/ERK, Src, and phosphatidylinositol 3-kinase/Akt controls cell migration and proliferation in human vascular pericytes. *J. Biol. Chem. 276:9945.*